

W boson mass in Singlet-Triplet Scotogenic dark matter model

Aditya Batra,^{1,*} ShivaSankar K.A.,^{1,†} Sanjoy Mandal,^{2,‡} and Rahul Srivastava^{1,§}

¹*Department of Physics, Indian Institute of Science Education and Research - Bhopal,
Bhopal Bypass Road, Bhauri, Bhopal 462066, India*

²*Korea Institute for Advanced Study, Seoul 02455, Korea*

The recent high precision measurement of W boson mass by CDF-II collaboration points to the contribution(s) of new physics beyond the Standard Model. One of the minimalistic ways to account for the anomalous W boson mass is by introducing a hyperchargeless real $SU(2)_L$ triplet scalar whose vacuum expectation value explicitly contributes to the W boson mass at the tree level while the Z boson mass remains the same. Such a triplet can be naturally embedded in a singlet-triplet scotogenic model for one loop neutrino mass generated by dark sector particles running in the loop. We discuss the detailed phenomenology of the model, obtaining the parameter space consistent with the CDF-II W boson mass measurements. The dark matter as well as the constraints coming from S , T , U parameters are also analyzed.

1. INTRODUCTION

Some of the main goals of Large Hadron Collider (LHC) have been to shed more light on the detailed mechanism of spontaneous symmetry breaking in the Standard Model (SM) and to look for possible new physics beyond Standard Model (BSM). The ATLAS [1] and CMS [2] experiments have partially fulfilled this aim with the discovery of a scalar particle of mass 125 GeV with properties that are similar to those of the SM Higgs. The discovery of neutrino oscillations [3] provides us with another important milestone in particle physics. At many scales, there has now been significant evidence for the presence of cosmic dark matter [4] whose deep understanding we still lack. Therefore, despite its outstanding achievements, it is now widely expected that the SM cannot be the final theory of nature.

Recently the CDF-II collaboration has reported their high precision measurement of W boson mass $M_W^{\text{CDF-II}} = 80.4335 \pm 0.0094$ GeV [5] which shows a $7\text{-}\sigma$ deviation from the SM expectation ($M_W^{\text{SM}} = 80.354 \pm 0.007$ GeV) [6]. Such a strong deviation from the SM prediction opens up the possibilities of studying new physics contributions to W boson mass [7–61].

* adityab17@iiserb.ac.in

† shivasankar17@iiserb.ac.in

‡ smandal@kias.re.kr

§ rahul@iiserb.ac.in

Of particular interest are new physics models which can relate the CDF-II anomaly with the other shortcomings of the SM such as the long standing open questions in neutrino and dark matter physics. In this article, we discuss such an extension which explains the CDF-II anomaly along with generating naturally small one loop masses for the neutrinos through a novel variant of the canonical scotogenic model [62]. The model contains a real $SU(2)_L$ triplet scalar whose vacuum expectation value (VEV) can modify the W boson mass without changing Z boson mass. We show that with only a triplet scalar one can explain the new CDF-II measurements at tree level itself. We further show that such a real triplet scalar is naturally embedded in a generalization of the scotogenic model initially proposed in [63, 64]. This simple models contains just a few new fields beyond the SM particle content: one singlet fermion N and one hyperchargeless $SU(2)_L$ triplet fermion Σ . These are odd under a \mathbb{Z}_2 dark symmetry. Moreover, we include two new scalars: one \mathbb{Z}_2 odd $SU(2)_L$ doublet η and the \mathbb{Z}_2 even $SU(2)_L$ triplet scalar Ω carrying no hypercharge. The advantage with this model is that the lack of neutrino mass and of a viable WIMP dark matter candidate, have a common origin. In addition we show that along with the small induced scalar triplet VEV, one gets additional contribution to the W boson mass through the loop quantum corrections quantified by the S , T and U parameters.

The plan of the paper is as follows. In Section 2 we present the modification of W boson mass from a tree level interaction with a real scalar $SU(2)_L$ triplet. In Section 3 we summarize the main properties of the model and discuss the singlet-triplet scotogenic model for neutrino mass generation. In Section 4 we discuss the S , T , U parameter space for the model in consideration with CDF-II results and compare it with the experimental constraints. In Section 5 we discuss the dark matter constraints for the case of the scalar dark matter. Finally, we summarize our results in Sec. 6.

2. REAL TRIPLET SCALAR CONTRIBUTION TO THE W MASS

Before discussing the singlet-triplet scotogenic model in details, in this section we briefly discuss the impact of adding a $SU(2)_L$ triplet scalar Ω with $U(1)_Y = 0$ to the particle content of the SM. The new interaction term relevant for W boson mass in the Lagrangian is given by

$$\mathcal{L}_\Omega = \text{Tr} [(D_\mu \Omega)^\dagger (D^\mu \Omega)], \quad \text{with } \Omega = \begin{pmatrix} \frac{\Omega^0}{\sqrt{2}} & \Omega^+ \\ \Omega^- & -\frac{\Omega^0}{2} \end{pmatrix} \quad (1)$$

where the covariant derivative D_μ is defined as

$$D_\mu \Omega = \partial_\mu \Omega + ig [W_\mu, \Omega] \quad (2)$$

with g being the weak coupling constant. After electroweak symmetry breaking both the $SU(2)_L$ doublet scalar Φ and triplet scalar Ω get VEVs

$$\langle\phi^0\rangle = \frac{v_\Phi}{\sqrt{2}}, \quad \langle\Omega^0\rangle = v_\Omega \quad (3)$$

With $v_\Omega \neq 0$, we can calculate the contribution of the triplet scalar to masses of gauge bosons. The masses of W and Z boson are given by,

$$M_W = \frac{g}{2}\sqrt{v_\Phi^2 + 4v_\Omega^2} \text{ and } M_Z = \frac{\sqrt{g^2 + g'^2}}{2}v_\Phi \quad (4)$$

where g' is the coupling constant associated with the $U(1)_Y$ gauge symmetry. Clearly, since Ω has zero hypercharge, it only contributes to the W boson mass. Accordingly, the ρ parameter modifies to

$$\rho = \frac{\sqrt{v_\Phi^2 + 4v_\Omega^2}}{v_\Phi} \approx 1 + 2\frac{v_\Omega^2}{v_\Phi^2} \quad (5)$$

Since, now the mass of W boson also depends on v_Ω , the new CDF-II measurement can be used to put “naive bounds” on v_Ω ¹. We can constrain v_Ω using the equation

$$M_{W,\text{CDF}}^2 - M_{W,\text{SM}}^2 = g^2v_\Omega^2 \quad (6)$$

where $M_{W,\text{SM}}^2 = g^2v_\Phi^2/4$ is the tree level value of the W boson mass in the SM.

One can use (6) to plot the tree level change in W boson mass with respect to the v_Ω as shown in Fig. 1. From Fig. 1 we can see that the mass of the W boson increases with the increase in the VEV of the triplet scalar. The purple shaded region is the $1\text{-}\sigma$ range of the W boson mass given by the Particle Data Group [65]. The $1\text{-}\sigma$ range of the new CDF-II measured is shown in dark orange color [5]. Considering the new CDF-II measurement and the SM prediction and requiring that the new W mass contribution comes from the VEV of Ω^0 , the constraint in equation (6) translates to a bound on the VEV given by

$$4.9 \text{ GeV} \lesssim v_\Omega \lesssim 6.0 \text{ GeV} \quad (7)$$

as indicated by the vertical green region in Fig. 1. Thus, the addition of the hyperchargeless real triplet scalar can easily modify the mass of the W boson consistent with CDF-II measured value without changing the Z boson mass. However, it will be much more interesting to see if such a scalar can be naturally connected to other experimental and observational shortcomings of the SM in an intimate and self consistent way. In the rest of the paper we discuss such a scenario where the real triplet scalar is naturally embedded in a simple model

¹ This naive bound is just for illustrative purposes in order to discuss the idea in a simplified setup. Of course the CDF-II or for that matter any experimental mass measurement cannot be directly equated to tree level theoretical values. We do a more careful analysis taking into account the impact of loop corrections and the resulting oblique parameters in later sections.

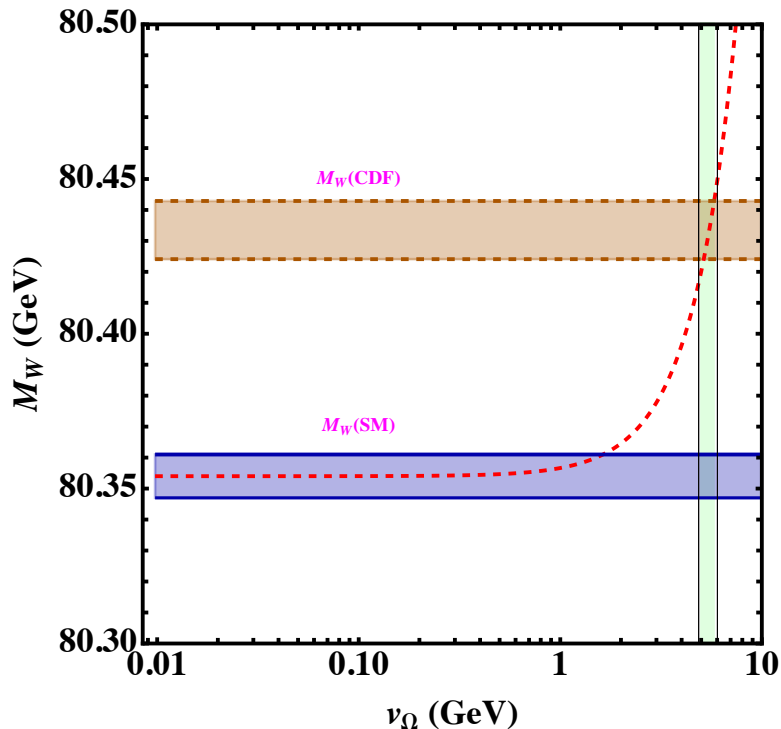


FIG. 1: The mass of W boson vs VEV v_Ω of the triplet scalar. The horizontal purple band corresponds to the SM prediction [6] while the dark orange band corresponds to the $1\text{-}\sigma$ limit from the CDF-II measurement [5]. The vertical green band denotes the range of v_Ω which is compatible with the CDF-II result.

for neutrino masses and dark matter.

3. THE SINGLET TRIPLET SCOTOGENIC MODEL

In this section we discuss the details of the singlet-triplet scotogenic model which generates small neutrino masses at one loop level with the dark matter running in the neutrino mass loop. The particle content of the model and their respective charges are given in Table I. The extended particle content includes three generations of singlet Majorana fermions N and hyperchargeless triplet Majorana fermions Σ , both of which are charged odd under a \mathbb{Z}_2 dark symmetry. In the scalar sector, apart from the Higgs doublet Φ , we have added an $SU(2)_L$ doublet scalar which is odd under \mathbb{Z}_2 and a real hyperchargeless $SU(2)_L$ triplet scalar Ω which is charged even under \mathbb{Z}_2 . Due to the \mathbb{Z}_2 symmetry conservation, the doublet scalar η should not acquire any VEV, resulting in the neutrino masses arising from a loop diagram as shown in Fig. 2. As we have discussed, the VEV of the neutral component of the triplet scalar Ω contributes also to the W boson mass.

The $SU(3)_c \otimes SU(2)_L \otimes U(1)_Y \otimes \mathbb{Z}_2$ invariant Yukawa Lagrangian for the particle content

Fields	$SU(3)_c \otimes SU(2)_L \otimes U(1)_Y$	\mathbb{Z}_2
L	$(1, 2, -\frac{1}{2})$	+1
ℓ	$(1, 1, -1)$	+1
Φ	$(1, 2, \frac{1}{2})$	+1
Σ	$(1, 3, 0)$	-1
N	$(1, 1, 0)$	-1
η	$(1, 2, \frac{1}{2})$	-1
Ω	$(1, 3, 0)$	-1

TABLE I: Particle content and charge assignments for singlet-triplet scotogenic model. The flavour indices are suppressed for brevity.

given in Table. I is

$$-\mathcal{L}_Y = Y_e^{\alpha\beta} \bar{L}_\alpha \Phi \ell_\beta + Y_N^\alpha \bar{L}_\alpha \tilde{\eta} N + Y_\Sigma^\alpha \bar{L}_\alpha C \Sigma^\dagger \tilde{\eta} + Y_\Omega \text{Tr}[\bar{\Sigma} \Omega] N + \frac{1}{2} M_\Sigma \text{Tr}[\bar{\Sigma}^c \Sigma] + \frac{1}{2} M_F \bar{N}^c N + \text{h.c.} \quad (8)$$

where $\alpha, \beta = 1, 2, 3$ are the flavour indices and $\tilde{\eta} = i\sigma_2 \eta^*$; σ_2 being the second Pauli matrix. For sake of brevity we have suppressed the flavour indices throughout this work unless explicitly stated. The scalar sector potential invariant under the $SU(3)_c \otimes SU(2)_L \otimes U(1)_Y \otimes \mathbb{Z}_2$ symmetry is given by

$$\begin{aligned} \mathcal{V} = & -m_\Phi^2 \Phi^\dagger \Phi + m_\eta^2 \eta^\dagger \eta + \frac{\lambda_1}{2} (\Phi^\dagger \Phi)^2 + \frac{\lambda_2}{2} (\eta^\dagger \eta)^2 + \lambda_3 (\Phi^\dagger \Phi) (\eta^\dagger \eta) + \lambda_4 (\Phi^\dagger \eta) (\eta^\dagger \Phi) \\ & + \frac{\lambda_5}{2} [(\Phi^\dagger \eta)^2 + \text{h.c.}] + \frac{m_\Omega^2}{2} \text{Tr}(\Omega^\dagger \Omega) + \frac{\lambda_1^\Omega}{2} (\Phi^\dagger \Phi) \text{Tr}(\Omega^\dagger \Omega) + \frac{\lambda_2^\Omega}{4} \text{Tr}(\Omega^\dagger \Omega)^2 \\ & + \frac{\lambda^\eta}{2} (\eta^\dagger \eta) \text{Tr}(\Omega^\dagger \Omega) + \mu_1 \Phi^\dagger \Omega \Phi + \mu_2 \eta^\dagger \Omega \eta. \end{aligned} \quad (9)$$

The spontaneous electroweak symmetry breaking will be driven by the neutral component of Φ and Ω . The field η can not acquire a VEV due to the conservation of \mathbb{Z}_2 symmetry. The $SU(2)_L$ doublets Φ , η and $SU(2)_L$ triplet Σ , Ω can be written as follows

$$\Phi = \begin{pmatrix} \phi^+ \\ \phi^0 \end{pmatrix}, \quad \eta = \begin{pmatrix} \eta^+ \\ \eta^0 \end{pmatrix}, \quad \Sigma = \begin{pmatrix} \frac{\Sigma^0}{\sqrt{2}} & \Sigma^+ \\ \Sigma^- & -\frac{\Sigma^0}{\sqrt{2}} \end{pmatrix} \quad \text{and} \quad \Omega = \begin{pmatrix} \frac{\Omega^0}{\sqrt{2}} & \Omega^+ \\ \Omega^- & -\frac{\Omega^0}{\sqrt{2}} \end{pmatrix}. \quad (10)$$

As already mentioned, the spontaneous electroweak symmetry breaking will be driven by the neutral components of Φ and Ω ,

$$\langle \phi^0 \rangle = \frac{v_\Phi}{\sqrt{2}}, \quad \langle \Omega^0 \rangle = v_\Omega, \quad \langle \eta^0 \rangle = 0, \quad (11)$$

Minimization of the total potential $\mathcal{V}(\Phi, \Omega, \eta)$ leads to the relations:

$$m_\Omega^2 = M_0^2 - \frac{\lambda_1^\Omega v_\Phi^2}{2} - \frac{\lambda_2^\Omega v_\Omega^2}{2}, \quad \text{with } M_0^2 \equiv \frac{v_\Phi^2 \mu_1}{2v_\Omega}. \quad (12)$$

$$m_\Phi^2 = \frac{v_\Phi^2 \lambda_1}{2} - \frac{\mu_1}{2} v_\Omega + \frac{\lambda_1^\Omega}{4} v_\Omega^2. \quad (13)$$

In the limit $M_0 \gg v_\Phi$, we can solve (12) for v_Ω . Keeping terms of $\mathcal{O}(v_\Phi/M_0)$ we get the small induced triplet vacuum expectation value :

$$\boxed{v_\Omega \approx \frac{\mu_1 v_\Phi^2}{2M_0^2}}. \quad (14)$$

providing a natural explanation for the smallness of the v_Ω consistent with the naive limits obtained in Sec.2 for the CDF-II measurements.

After electroweak symmetry breaking there are three physical CP-even neutral fields and one CP-odd neutral field as one of them is absorbed by the Z gauge boson. Also, there are three charged scalars, among them two are physical and one of them is absorbed by the W gauge boson. The mass matrix of CP-even neutral scalars in the basis (h^0, Ω^0) reads as

$$\mathcal{M}_S^2 = \begin{pmatrix} \lambda_1 v_\Phi^2 & \lambda_1^\Omega v_\Omega v_\Phi - \mu_1 \frac{v_\Phi}{\sqrt{2}} \\ \lambda_1^\Omega v_\Omega v_\Phi - \mu_1 \frac{v_\Phi}{\sqrt{2}} & 2\lambda_2^\Omega v_\Omega^2 + \frac{\mu_1}{2\sqrt{2}} \frac{v_\Phi^2}{v_\Omega} \end{pmatrix} \equiv \begin{pmatrix} A & B \\ B & C \end{pmatrix} \quad (15)$$

with the mass eigenvalues given as

$$m_{h,H}^2 = \frac{1}{2}(A + C \mp \sqrt{(A - C)^2 + 4B^2}) \quad (16)$$

where we will identify the h as SM-like Higgs boson discovered at LHC [66, 67]. The mass matrix for the charged scalars in the basis (ϕ^\pm, Ω^\pm) is given as

$$\mathcal{M}_{H^\pm}^2 = \begin{pmatrix} \sqrt{2}\mu_1 v_\Omega & \mu_1 \frac{v_\Phi}{\sqrt{2}} \\ \mu_1 \frac{v_\Phi}{\sqrt{2}} & \mu_1 \frac{v_\Phi^2}{2\sqrt{2}v_\Omega} \end{pmatrix}.$$

where the zero eigenvalue eigenstate corresponds to the would be Goldstone boson of the charged gauge boson W^\pm . The other is a physical charged scalar which has mass

$$m_{H^\pm}^2 = \frac{\mu_1(v_\Phi^2 + 4v_\Omega^2)}{2\sqrt{2}v_\Omega} \quad (17)$$

As the charged Goldstone boson is a linear combination of ϕ^+ and Ω^+ , the VEV of Ω will contribute to the W boson mass as follows,

$$M_W^2 = \frac{1}{4} g^2 (v_\Phi^2 + 4v_\Omega^2), \quad (18)$$

Finally the masses of η doublet components can be written as follows

$$m_{\eta_R}^2 = m_\eta^2 + \frac{1}{2}(\lambda_3 + \lambda_4 + \lambda_5)v_\Phi^2 + \frac{1}{2}\lambda^\eta v_\Omega^2 - \frac{1}{\sqrt{2}}v_\Omega\mu_2 \quad (19)$$

$$m_{\eta_I}^2 = m_\eta^2 + \frac{1}{2}(\lambda_3 + \lambda_4 - \lambda_5)v_\Phi^2 + \frac{1}{2}\lambda^\eta v_\Omega^2 - \frac{1}{\sqrt{2}}v_\Omega\mu_2 \quad (20)$$

$$m_{\eta^\pm}^2 = m_\eta^2 + \frac{1}{2}\lambda_3 v_\Phi^2 + \frac{1}{2}\lambda^\eta v_\Omega^2 + \frac{1}{\sqrt{2}}v_\Omega\mu_2. \quad (21)$$

For later convenience we define the ‘‘mean mass’’ $m_{\eta^0}^2 = (m_{\eta_R}^2 + m_{\eta_I}^2)/2$. The mass difference $m_{\eta_R}^2 - m_{\eta_I}^2$ depends only on λ_5 , which as we show later, is also responsible for the smallness of the neutrino mass scale. Thus, the smallness of the neutrino masses implies that λ_5 is quite small which in turn implies that η_R and η_I are almost mass degenerate.

Neutrino masses

The light neutrino masses are generated by the singlet-triplet scotogenic loop as shown in Fig. 2, which can explain the small neutrino masses. The real triplet scalar whose VEV can account for the W boson mass anomaly plays a crucial role in the case of neutrino mass generation.

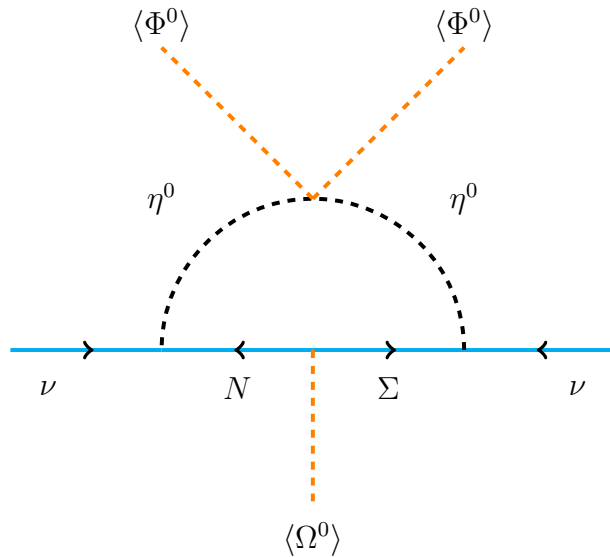


FIG. 2: One loop neutrino mass in the singlet-triplet scotogenic model, where $\eta^0 = (\eta_R, \eta_I)$.

Through the term proportional to the Yukawa coupling Y_Ω given in (8), the triplet scalar generates a mixing between the singlet and triplet fermion fields N and Σ . As a result, one

gets the following tree level fermion masses

$$m_{\chi^\pm} = M_\Sigma \quad (22)$$

$$m_{\chi_1} = \frac{1}{2} \left((M_\Sigma + M_N) - \sqrt{(M_\Sigma - M_N)^2 + 4Y_\Omega^2 v_\Omega^2} \right) \quad (23)$$

$$m_{\chi_2} = \frac{1}{2} \left((M_\Sigma + M_N) + \sqrt{(M_\Sigma - M_N)^2 + 4Y_\Omega^2 v_\Omega^2} \right) \quad (24)$$

The mass eigenstates $\chi_{1,2}$ are determined by the 2×2 orthogonal matrix $V(\alpha)$,

$$\begin{pmatrix} \chi_1 \\ \chi_2 \end{pmatrix} = \begin{pmatrix} \cos \alpha & \sin \alpha \\ -\sin \alpha & \cos \alpha \end{pmatrix} \begin{pmatrix} \Sigma^0 \\ N \end{pmatrix} = V(\alpha) \begin{pmatrix} \Sigma^0 \\ N \end{pmatrix}, \quad (25)$$

with

$$\tan(2\alpha) = \frac{2Y_\Omega v_\Omega}{M_\Sigma - M_N}. \quad (26)$$

It is interesting to notice that due to the \mathbb{Z}_2 symmetry conservation, the lightest neutral eigenstate, χ_1 or χ_2 may also play the role of the dark matter [63].

The expression for the neutrino mass matrix is

$$(\mathcal{M}_\nu)_{\alpha\beta} = \sum_{\sigma=1}^2 \left(\frac{ih_{\alpha\sigma}}{\sqrt{2}} \right) \left(\frac{-ih_{\beta\sigma}}{\sqrt{2}} \right) \frac{m_{\chi_\sigma}}{(4\pi)^2} \left[\frac{m_{\eta_R}^2 \ln \left(\frac{m_{\chi_\sigma}^2}{m_{\eta_R}^2} \right)}{m_{\chi_\sigma}^2 - m_{\eta_R}^2} - \frac{m_{\eta_I}^2 \ln \left(\frac{m_{\chi_\sigma}^2}{m_{\eta_I}^2} \right)}{m_{\chi_\sigma}^2 - m_{\eta_I}^2} \right] \quad (27)$$

where h is a 3×2 matrix defined as

$$h = \begin{pmatrix} \frac{Y_\Sigma^1}{\sqrt{2}} & Y_N^1 \\ \frac{Y_\Sigma^2}{\sqrt{2}} & Y_N^2 \\ \frac{Y_\Sigma^3}{\sqrt{2}} & Y_N^3 \end{pmatrix} \cdot V^T(\alpha), \quad (28)$$

It proves convenient to write the neutrino mass matrix in Eq. (27) as

$$\mathcal{M}_\nu = h \Lambda h^T \quad (29)$$

where

$$\Lambda = \begin{pmatrix} \Lambda_1 & 0 \\ 0 & \Lambda_2 \end{pmatrix}, \quad \Lambda_\sigma = \frac{m_{\chi_\sigma}}{2(4\pi)^2} \left[\frac{m_{\eta_R}^2 \ln \left(\frac{m_{\chi_\sigma}^2}{m_{\eta_R}^2} \right)}{m_{\chi_\sigma}^2 - m_{\eta_R}^2} - \frac{m_{\eta_I}^2 \ln \left(\frac{m_{\chi_\sigma}^2}{m_{\eta_I}^2} \right)}{m_{\chi_\sigma}^2 - m_{\eta_I}^2} \right]. \quad (30)$$

In order to compare with the current determination of neutrino oscillation parameters [68], we will apply a Casas-Ibarra parametrization [69] as follows

$$h = U^* \sqrt{\widehat{\mathcal{M}}_\nu} R \sqrt{\Lambda}^{-1}. \quad (31)$$

Here R is a 3×2 complex matrix such that $RR^T = \mathbb{I}_3$, $\widehat{\mathcal{M}}_\nu$ is the diagonal neutrino mass matrix and U is the leptonic mixing matrix.

4. THE W BOSON MASS AND S, T AND U PARAMETERS

In the SM, the W boson mass can be calculated very precisely in terms of the precisely measured input parameters $\{G_F, \alpha_{\text{em}}, M_Z, m_h, m_t, \alpha_s(M_Z)\}$. The W boson mass is related with these parameters in the following way:

$$M_W = \frac{M_Z}{2} \left(1 + \sqrt{1 - \frac{4\pi\alpha_{\text{em}}}{\sqrt{2}G_F M_Z^2 (1 - \Delta r)}} \right), \quad (32)$$

where Δr represents the quantum corrections. Note that here the M_W and M_Z are the renormalized masses in the on-shell scheme. Taking the central values of the input parameters, $M_Z = 91.1876$ GeV, $\alpha_{\text{em}}^{-1}(0) = 137.036$, $s_W^2 = 0.2315$, $M_t = 172.76$ GeV, $M_h = 125.25$ GeV, and $G_F = 1.1663787 \times 10^{-5}$ GeV⁻², one finds from Eq. (32) $M_W = 80.354$ GeV, which is $7\text{-}\sigma$ below the CDF-II measurement [5].

Provided that the new physics mass scale is higher than the electroweak scale, and that it contributes only through virtual loops to the electroweak precision observables, the dominant BSM effects can be parametrised by three gauge boson self-energy parameters named the oblique parameters S, T and U . These can be considered as the reparametrisations of the variables $\Delta\rho$, $\Delta\kappa$ and Δr , which absorb the radiative corrections to the total Z coupling strength, the effective weak mixing angle, and the W mass, respectively. For a given new physics model, the S, T, U predictions consist of the sum of the BSM contributions and the non-vanishing SM remainders when the m_h and m_t values differ from those used for the SM reference. The deviation of M_W^{CDF} from its SM prediction can be parameterized in terms of the oblique parameters, S, T and U as follows:

$$M_W = M_W^{\text{SM}} \left[\frac{\sqrt{v_\Phi^2 + 4v_\Omega^2}}{v_\Phi} - \frac{\alpha_{\text{em}}}{4(c_W^2 - s_W^2)} (S - 1.55T - 1.24U) \right] \quad (33)$$

where the first term comes from the tree level contribution of the triplet scalar VEV while all BSM particles contribute through loops to the S, T, U parameters².

Recently, Ref. [8] gave the values of these parameters from an analysis of precision electroweak data including the CDF-II new result of the W -mass:

$$S = 0.06 \pm 0.10, \quad T = 0.11 \pm 0.12 \quad \text{and} \quad U = 0.14 \pm 0.09, \quad (34)$$

² In a given model, the contribution of different BSM particles to S, T, U parameters need not be of equal importance.

with the correlation

$$\rho_{ST} = 0.90, \quad \rho_{SU} = -0.59 \quad \text{and} \quad \rho_{TU} = -0.85. \quad (35)$$

On the other hand, since the values of the U parameter are found to be very small in many new physics models, it is reasonable to consider $U \approx 0$. With this assumption, Ref. [8] found the following values of S and T :

$$S = 0.15 \pm 0.08 \quad \text{and} \quad T = 0.27 \pm 0.06 \quad \text{with the correlation} \quad \rho_{ST} = 0.93 \quad (36)$$

4.1. S, T, U parameters in singlet-triplet scotogenic model

Since the scalar triplet (Ω), scalar doublet (η) and triplet fermion (Σ) couple to the $SU(2)_L$ gauge bosons, they can potentially affect the oblique parameters S, T, U through loop corrections. The contributions to S, T, U are given by [70–72]

$$\begin{aligned}
 S &\simeq \underbrace{\frac{1}{12\pi} \log \left(\frac{m_{\eta^0}^2}{m_{\eta^+}^2} \right)}_{\text{Scalar doublet contribution}} + \frac{1}{18\pi} \\
 T &\simeq \underbrace{\frac{1}{6\pi} \frac{1}{\sin^2(\theta_W)} \frac{1}{\cos^2(\theta_W)} \frac{\Delta M}{M_Z^2}}_{\text{Scalar triplet contribution}} + \underbrace{\frac{2\sqrt{2}G_F}{(4\pi)^2\alpha_{em}} \left[\frac{m_{\eta^0}^2 + m_{\eta^+}^2}{2} - \frac{m_{\eta^0}^2 m_{\eta^+}^2}{m_{\eta^+}^2 - m_{\eta^0}^2} \log \left(\frac{m_{\eta^+}^2}{m_{\eta^0}^2} \right) \right]}_{\text{Scalar doublet contribution}} \\
 U &\simeq \underbrace{\frac{\Delta M}{3\pi M_H^\pm}}_{\text{Scalar triplet contribution}} \\
 &+ \underbrace{\frac{1}{12\pi} \left[-\frac{5m_{\eta^+}^4 - 22m_{\eta^+}^2 m_{\eta^0}^2 + 5m_{\eta^0}^4}{3(m_{\eta^+}^2 - m_{\eta^0}^2)^2} + \frac{(m_{\eta^+}^2 + m_{\eta^0}^2)(m_{\eta^+}^4 - 4m_{\eta^+}^2 m_{\eta^0}^2 + m_{\eta^0}^4)}{(m_{\eta^+}^2 - m_{\eta^0}^2)^3} \right]}_{\text{Scalar doublet contribution}}
 \end{aligned} \quad (37)$$

where $\Delta M = M_{\Omega^\pm} - M_{\Omega^0}$ corresponds to the mass splitting between the charged and neutral components of the triplet scalar Ω . This mass splitting is directly proportional to the triplet VEV v_Ω . Due to the smallness of the triplet VEV, $\Delta M \ll M_Z$. This in turn implies that the triplet scalar contribution to the S, T, U parameters will be negligibly small compared to the contribution coming from the doublet scalar η , a fact which we have also verified numerically. Furthermore, since the triplet fermion Σ has an invariant Majorana mass term, its mass is independent of the electroweak scale and is typically taken to be much larger than the electroweak scale. Thus, in writing the above relations, we have ignored the contribution of the Σ as its contribution is expected to be negligibly small. Finally, the SM gauge singlet fermion N also has a large invariant mass and in addition, being a gauge singlet it obviously

does not contribute to the S , T , U parameters.

Thus, in the end there are primarily two different important contributions to the mass of the W boson in our model:

1. The direct tree level contribution of the triplet scalar through its VEV v_Ω .
2. The loop level contribution of the doublet scalar η .

Being two independent sources, in our model both or only one of them can be the dominant contribution leading to the W boson mass in agreement with CDF-II measurement. In previous section we have already discussed the scenario where the triplet scalar contribution is the dominant contribution. Here, we want to explore the scenario where v_Ω is much smaller than the GeV scale so that its contribution to W mass is negligible. In such a case, the BSM contribution to W mass is purely coming from quantum loop corrections, i.e., only through the S , T and U parameters. In such a case the CDF-II measurements imply a strong correlation between the masses of the charged and neutral components of the doublet scalar η as shown in Fig.3 with the color bar indicating the mass splitting $\Delta m_\eta = m_{\eta^+} - m_{\eta^0}$ between the charged and neutral components.

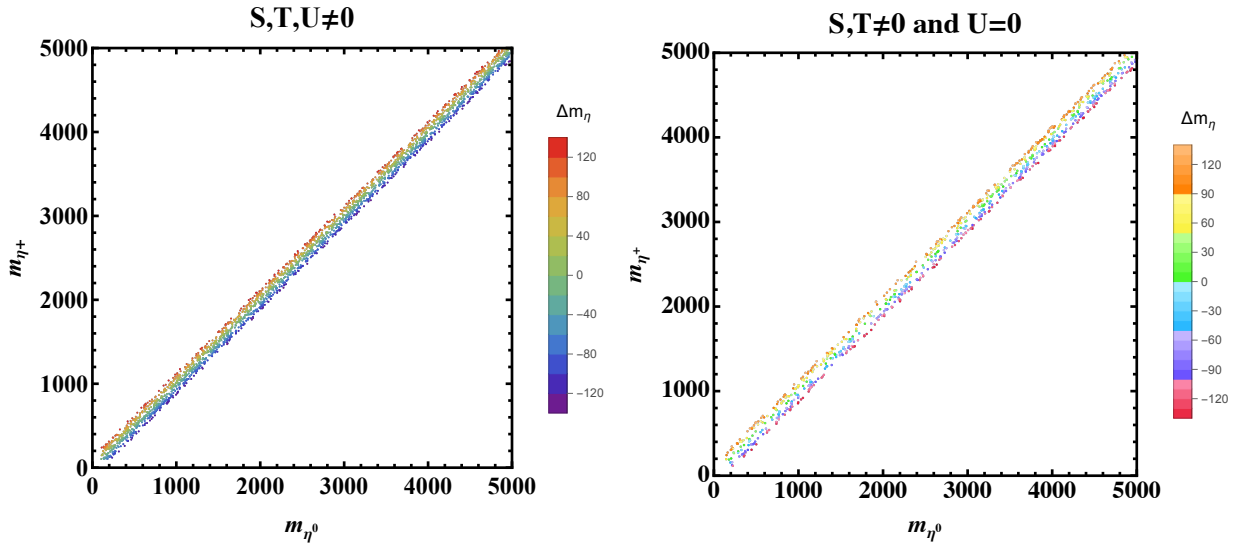


FIG. 3: Values of m_{η^0} vs m_{η^+} with the mass splitting Δm_η allowed by the new S , T , U parameter space as given in [8]. The left panel is with $S, T, U \neq 0$ and the right panel is for $S, T \neq 0, U = 0$. See text for details.

As mentioned above, the dominant contributions to W mass in this case is assumed to come from the doublet scalar. This allows us to constrain the parameter space of allowed values of masses of m_{η^0} and m_{η^+} that can simultaneously satisfy the S , T and U constraints for the new CDF-II data [8]. Since the contribution of doublet scalar to S , T , U are highly sensitive to the mass and mass differences of the charged and neutral components of the doublets as can be seen in (37), the allowed parameter space is a narrow band as shown

in 3. The narrow bands are also color coded with respect to the mass differences of the neutral and charged components of doublet scalar to better understand the sensitivity to mass differences. We can infer a maximum allowed value for the mass difference Δm_η to be around 120 GeV to satisfy the S , T and U constraints.

5. DARK MATTER CONSTRAINTS

In this section we collect the results of our dark matter analysis. Since both N and Σ fermions have invariant mass terms which can be much larger than the electroweak scale, we have assumed them to be heavy. With this assumption, the \mathbb{Z}_2 symmetry conservation makes the lightest of the two scalar eigenstates η_R and η_I a viable dark matter candidate. In our analysis we take η_R as the dark matter candidate with $\lambda_5 < 0$ (the opposite scenario with $\lambda_5 > 0$ would have η_I as the dark matter candidate). We implemented the model in SARAH [73] and SPheno [74] to calculate all the vertices, mass matrices, tadpole equations, whereas the thermal component of the dark matter relic, as well as dark matter direct detection cross sections are determined by micrOMEGAS-5.0.8 [75].

Scalar Dark matter - η_R	
Parameter	Range
m_η^2	$[10^2, 2.5 \times 10^7]$ GeV
M_Σ, M_N	$[m_{\eta_R} + 10, m_{\eta_R} + 5000]$ GeV
μ_i	$[10, 3000]$ GeV
v_Ω	$[2, 6]$ GeV
λ_5	$[-10^{-5}, -10^{-1}]$
λ_4	$[-\lambda_5 - 10^{-5}, -\lambda_5 - 10^{-1}]$
λ_2, λ_3	$[10^{-5}, 10^{-1}]$
λ_i^Ω	$[10^{-5}, 10^{-1}]$
λ^η	$[10^{-5}, 10^{-1}]$
Y_Ω	$[10^{-5}, 10^{-1}]$
Y_ν	$[10^{-5}, 10^{-1}]$

TABLE II: Value range for the numerical parameter scan for a scalar dark matter candidate.

We show in Fig. 4, the behaviour of relic density as a function of the mass of the scalar dark matter candidate η_R . The narrow band is the $3\text{-}\sigma$ allowed range for relic density [4]: $0.1126 \leq \Omega_{\eta_R} h^2 \leq 0.1246$. Our numerical scan was performed varying the input parameters as given in Table. II, assuming logarithmic steps. The range of m_η is taken to be 10 to 5000 GeV. The mass differences $m_\Sigma - m_{\eta_R}$ and $m_N - m_{\eta_R}$ each have a range of 10 to 5000 GeV. λ_1 is fixed in such a way that the lighter neutral CP-even scalar h has a mass of 125.25 ± 0.17 GeV [6]. The condition $\lambda_4 + \lambda_5 < 0$ is imposed such that $m_{\eta_R} < m_{\eta^\pm}$. The meaning of color

code in Fig. 4 is as follows: the cyan points are within the $3\text{-}\sigma$ range, whereas the blue and gray points are above and below the $3\text{-}\sigma$ range respectively.

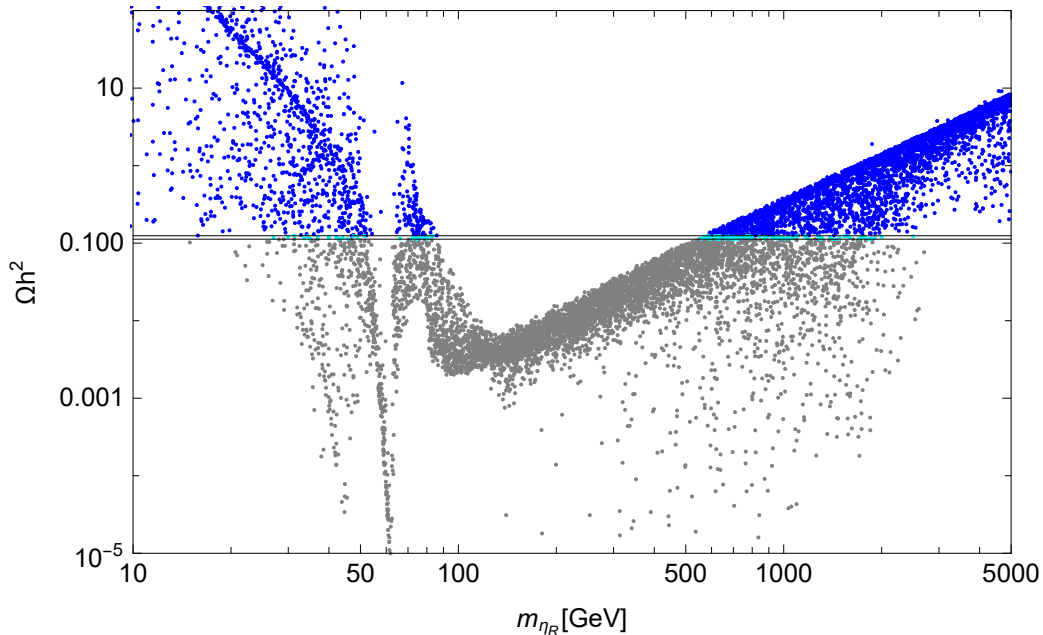


FIG. 4: Relic density versus the mass of the dark matter candidate m_{η_R} for various input parameters as given in Table. II. The cyan points are within the $3\text{-}\sigma$ range of observed relic density [4], whereas the blue and gray points correspond to over-abundant and under-abundant dark matter respectively.

The reasons for the various dips can be understood by looking in detail into the η_R annihilation and co-annihilation channels given in Fig. 6 in Appendix B. The first dip at $m_{\eta_R} \sim M_Z/2$ is due to annihilation and co-annihilation via s-channel Z -exchange. The second dip around $m_{\eta_R} \sim 60$ GeV corresponds to efficient annihilations via s-channel Higgs exchange. Note that some of the points in this dip can also be ruled out from the current collider limits on $\text{BR}(h \rightarrow \text{inv})$. The Higgs-exchange dip is more efficient than the Z -mediated one as Z -mediated channel is momentum suppressed. For heavier η_R masses, quartic interactions with gauge bosons starts contributing. For example, with $m_{\eta_R} \geq 80$ GeV, annihilations of η_R into W^+W^- and ZZ via quartic couplings are particularly important, hence the third drop in the relic abundance. For $m_{\eta_R} \geq 120$ GeV and $m_{\eta_R} \geq m_t$ GeV, η_R can annihilate also into two Higgs bosons, hh and $t\bar{t}$, respectively. For large m_{η_R} , the relic density increases due to the suppressed annihilation cross section, which drops as $\sim 1/m_{\eta_R}^2$. Notice also that when λ_5 is small, coannihilation channels with both η_I and η^\pm may occur in all regions of the parameter space.

The tree-level spin-independent η_R -nucleon cross section is mediated by the Higgs and the Z -portals as seen in Fig. 7 in Appendix B. For non-zero λ_5 , there is a small mass splitting between η_I and η_R , so the interaction through the Z -boson is kinematically forbidden or leads

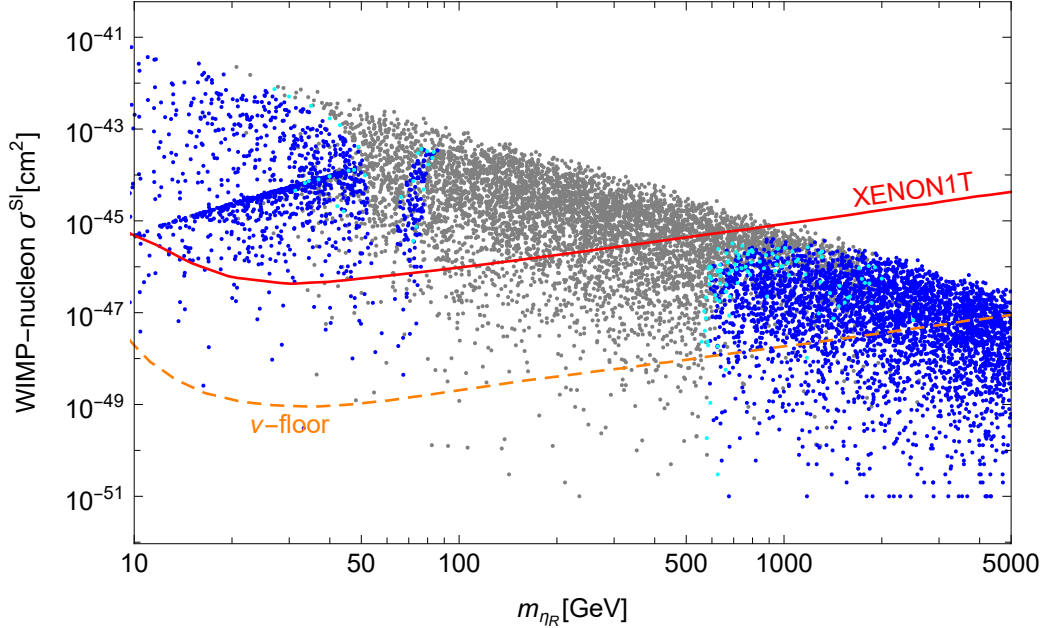


FIG. 5: Spin-independent WIMP-nucleon cross section versus the mass of the dark matter candidate m_{η_R} for various input parameters as given in Table. II. The color scheme is the same as in Fig. 4. The red line denotes the latest upper bound from the XENON1T collaboration [76] and the dashed orange line corresponds to the “neutrino floor” lower limit [77, 78].

to inelastic scattering, hence can be neglected compared to the Higgs-exchange contribution.

In Fig. 5, we show the direct detection prospects of our dark matter η_R , for the range of parameters covered by our scan given in Table. II. The color code of displayed points is the same as in Fig. 4. The red line denotes the latest upper bound from the XENON1T collaboration [76]. There are constraints from other experiments as well, such as LUX [79] and PandaX-II [80], but weaker when compared to the XENON1T limit. We also show the lower limit corresponding to the “neutrino floor” from coherent elastic neutrino scattering [77, 78]. We see from Fig. 5 that all the low-mass solutions with the correct dark matter relic density are ruled out by the XENON1T direct detection cross section upper limits.

Although we have taken the dark sector fermions of the model to be heavier than the dark scalars but this need not be the case. The fermionic dark matter in this model is also very interesting. In this case the relic abundance of Σ^0 is determined by the annihilation and co-annihilation of itself and Σ^\pm . These processes force the triplet dark matter mass to be in the range 2.3 TeV to 2.4 TeV. Also the direct detection only occurs through a loop. On the other hand, for pure singlet N , the dark matter mass can be much smaller compared to the pure triplet case. The main signature of N is the annihilation into neutrinos and charged leptons. Again, the disadvantage is that direct detection occurs only at the one loop level. Finally, note that the nonzero VEV of the scalar triplet Ω induces a mixing between Σ^0 and

N . If the Yukawa coupling between N and Σ through Ω is large, then the fermionic dark matter candidate χ_i can be a mixed state between N and Σ^0 . In comparison to models with only singlets or triplets, this interaction results in an enhanced dark matter phenomenology. This same mixing can also give tree-level direct detection. Unlike the pure singlet or pure triplet case, the singlet-triplet mixed dark matter has the best features of singlet-only or triplet-only scenarios with a better prospect of direct detection. For a detailed discussion on fermionic dark matter, we refer to [63].

6. CONCLUSIONS

We have presented a singlet-triplet scotogenic dark matter model to generate tiny neutrino masses at one loop level. In this model, the dark sector particles run in the loop generating the neutrino masses. The particle content of the model is simple. Apart from SM particles the model contains the SM gauge singlet fermion N and well as the hypercharge zero $SU(2)_L$ triplet fermion Σ along with the $SU(2)_L$ doublet scalar η . Additionally a hypercharge zero $SU(2)_L$ triplet scalar Ω is needed in order to complete the neutrino mass loop diagram. We looked at the prospects of the model satisfying the recent W boson mass measurements by the CDF-II collaboration. In the model there are two main corrections to the SM value of W mass, namely, direct modification due to the VEV v_Ω of the triplet scalar and loop corrections due to presence of the dark scalar η . We have analyzed both these possibilities. We find that the CDF-II result can be explained in both scenarios. We derived the resulting constraints on the VEV of the triplet scalar as well as the mass spectra of the doublet scalar components. Finally we looked at the dark matter phenomenology in the model and showed that the dark matter in our model indeed satisfies both the relic abundance and direct detection constraints over a large range of the parameter space.

ACKNOWLEDGMENTS

The work of RS is supported by the Government of India, SERB Startup Grant SRG/2020/002303. The work of S.M. is supported by KIAS Individual Grants (PG086001) at Korea Institute for Advanced Study.

Appendix A: Definition of S , T and U parameters

Following closely the notation by Peskin and Takeuchi in [81], the S , T and U parameters can be defined as

$$\alpha S \equiv 4e^2 \frac{d}{dp^2} [\Pi_{33}(p^2) - \Pi_{3Q}(p^2)] \Big|_{p^2=0}, \quad (\text{A1a})$$

$$\alpha T \equiv \frac{e^2}{s_W^2 c_W^2 m_Z^2} [\Pi_{11}(0) - \Pi_{33}(0)], \quad (\text{A1b})$$

$$\alpha U \equiv 4e^2 \frac{d}{dp^2} [\Pi_{11}(p^2) - \Pi_{33}(p^2)] \Big|_{p^2=0}, \quad (\text{A1c})$$

where $\alpha = e^2/4\pi$. $\Pi_{IJ} \equiv \Pi_{IJ}(p^2)$ are the various vacuum polarisation diagrams where I and J may be photon (γ), W or Z ,

$$\Pi_{\gamma\gamma} = e^2 \Pi_{QQ}, \quad (\text{A2a})$$

$$\Pi_{Z\gamma} = \frac{e^2}{c_W s_W} (\Pi_{3Q} - s^2 \Pi_{QQ}), \quad (\text{A2b})$$

$$\Pi_{ZZ} = \frac{e^2}{c_W^2 s_W^2} (\Pi_{33} - 2s^2 \Pi_{3Q} + s^4 \Pi_{QQ}), \quad (\text{A2c})$$

$$\Pi_{WW} = \frac{e^2}{s_W^2} \Pi_{11}, \quad (\text{A2d})$$

where $s_W = \sin \theta_W$, $c_W = \cos \theta_W$.

Appendix B: Feynman diagrams for dark matter relic density and direct detection

We show some of the most important Feynman diagrams for determining the cosmological relic density, assuming η^R is the dark matter. The primary dark matter annihilation and coannihilation channels are depicted in Fig. 6. Coannihilations with both η^I and η^\pm are feasible in addition to the standard s -wave annihilation into quarks and gauge bosons, which is mediated by the SM like Higgs boson. The Z boson, as well as the new fermions, can mediate these interactions. At the tree level, the diagrams in Fig. 7 contribute to the spin-independent η^R -nucleon elastic scattering cross section. Only when the separation between the masses of η^R and η^I is minimal (small λ_5 values) diagram on the right matter and leads to inelastic cross section.

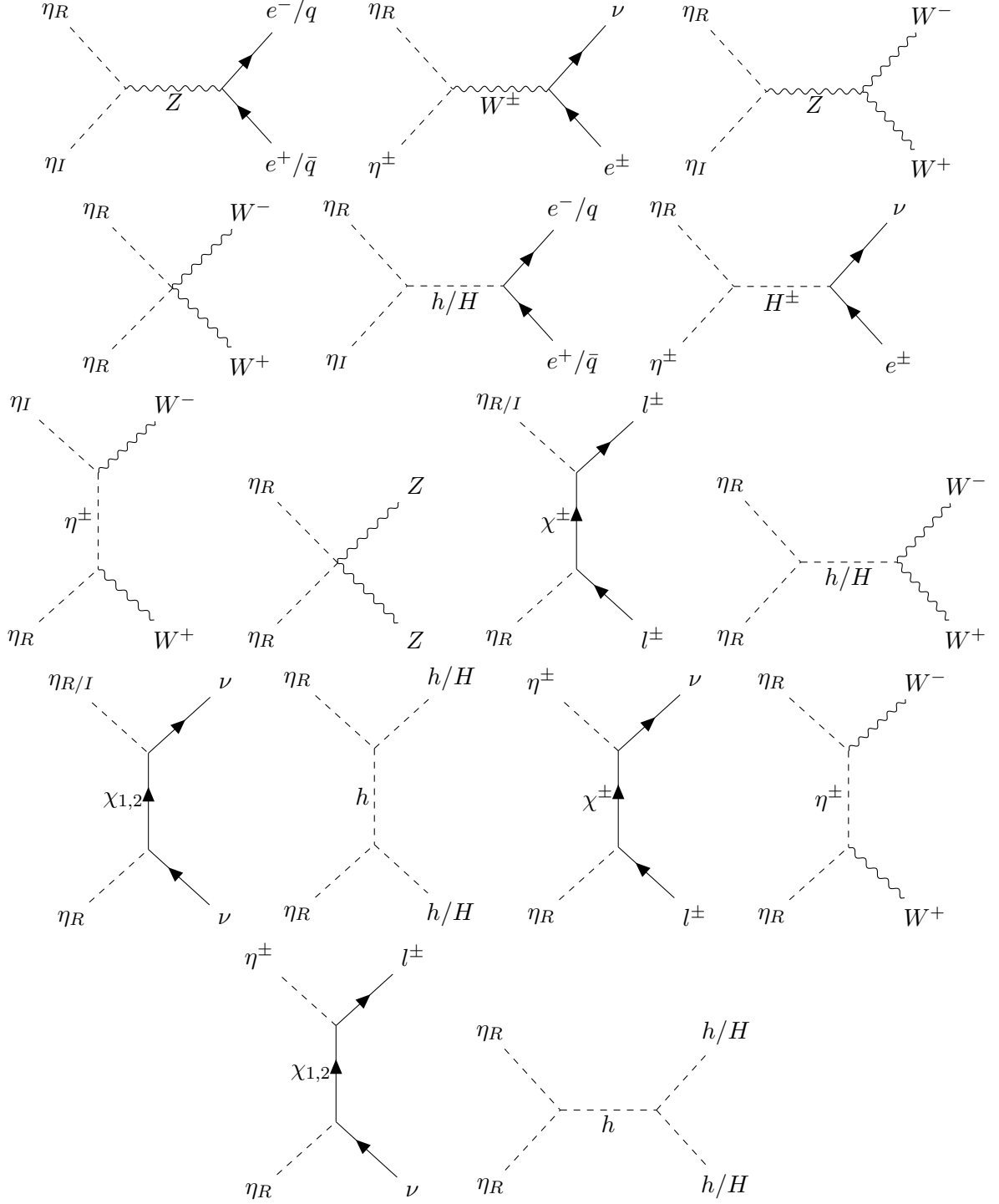


FIG. 6: Annihilation and co-annihilation Feynman diagrams that contribute to the relic density of η_R .

[1] **ATLAS** Collaboration, G. Aad *et al.*, “Observation of a new particle in the search for the

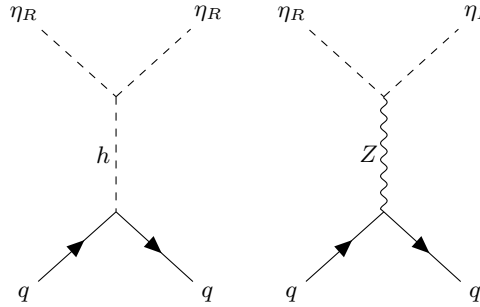


FIG. 7: η_R -nucleon scattering Feynman diagrams relevant for direct detection.

- Standard Model Higgs boson with the ATLAS detector at the LHC,” *Phys. Lett.* **B716** (2012) 1–29, [arXiv:1207.7214 \[hep-ex\]](#).
- [2] CMS Collaboration, S. Chatrchyan *et al.*, “Observation of a new boson at a mass of 125 GeV with the CMS experiment at the LHC,” *Phys. Lett.* **B716** (2012) 30–61, [arXiv:1207.7235 \[hep-ex\]](#).
- [3] Super-Kamiokande Collaboration, Y. Fukuda *et al.*, “Evidence for oscillation of atmospheric neutrinos,” *Phys. Rev. Lett.* **81** (1998) 1562–1567, [arXiv:hep-ex/9807003](#).
- [4] Planck Collaboration, N. Aghanim *et al.*, “Planck 2018 results. VI. Cosmological parameters,” *Astron. Astrophys.* **641** (2020) A6, [arXiv:1807.06209 \[astro-ph.CO\]](#). [Erratum: *Astron. Astrophys.* 652, C4 (2021)].
- [5] CDF Collaboration, T. Aaltonen *et al.*, “High-precision measurement of the W boson mass with the CDF II detector,” *Science* **376** no. 6589, (2022) 170–176.
- [6] Particle Data Group Collaboration, P. Zyla *et al.*, “Review of Particle Physics,” *PTEP* **2020** no. 8, (2020) 083C01. and 2021 update.
- [7] Y.-Z. Fan, T.-P. Tang, Y.-L. S. Tsai, and L. Wu, “Inert Higgs Dark Matter for New CDF W -boson Mass and Detection Prospects,” [arXiv:2204.03693 \[hep-ph\]](#).
- [8] C.-T. Lu, L. Wu, Y. Wu, and B. Zhu, “Electroweak Precision Fit and New Physics in light of W Boson Mass,” [arXiv:2204.03796 \[hep-ph\]](#).
- [9] P. Athron, A. Fowlie, C.-T. Lu, L. Wu, Y. Wu, and B. Zhu, “The W boson Mass and Muon $g - 2$: Hadronic Uncertainties or New Physics?,” [arXiv:2204.03996 \[hep-ph\]](#).
- [10] G.-W. Yuan, L. Zu, L. Feng, and Y.-F. Cai, “ W -boson mass anomaly: probing the models of axion-like particle, dark photon and Chameleon dark energy,” [arXiv:2204.04183 \[hep-ph\]](#).
- [11] A. Strumia, “Interpreting electroweak precision data including the W -mass CDF anomaly,” [arXiv:2204.04191 \[hep-ph\]](#).
- [12] J. M. Yang and Y. Zhang, “Low energy SUSY confronted with new measurements of W -boson mass and muon $g-2$,” [arXiv:2204.04202 \[hep-ph\]](#).
- [13] J. de Blas, M. Pierini, L. Reina, and L. Silvestrini, “Impact of the recent measurements of the top-quark and W -boson masses on electroweak precision fits,” [arXiv:2204.04204](#)

- [hep-ph].
- [14] C.-R. Zhu, M.-Y. Cui, Z.-Q. Xia, Z.-H. Yu, X. Huang, Q. Yuan, and Y. Z. Fan, “GeV antiproton/gamma-ray excesses and the W -boson mass anomaly: three faces of $\sim 60 - 70$ GeV dark matter particle?,” [arXiv:2204.03767 \[astro-ph.HE\]](#).
- [15] X. K. Du, Z. Li, F. Wang, and Y. K. Zhang, “Explaining The Muon $g - 2$ Anomaly and New CDFII W -Boson Mass in the Framework of ExtraOrdinary Gauge Mediation,” [arXiv:2204.04286 \[hep-ph\]](#).
- [16] T.-P. Tang, M. Abdughani, L. Feng, Y.-L. S. Tsai, and Y.-Z. Fan, “NMSSM neutralino dark matter for W -boson mass and muon $g - 2$ and the promising prospect of direct detection,” [arXiv:2204.04356 \[hep-ph\]](#).
- [17] G. Cacciapaglia and F. Sannino, “The W boson mass weighs in on the non-standard Higgs,” [arXiv:2204.04514 \[hep-ph\]](#).
- [18] M. Blennow, P. Coloma, E. Fernández-Martínez, and M. González-López, “Right-handed neutrinos and the CDF II anomaly,” [arXiv:2204.04559 \[hep-ph\]](#).
- [19] K. Sakurai, F. Takahashi, and W. Yin, “Singlet extensions and W boson mass in the light of the CDF II result,” [arXiv:2204.04770 \[hep-ph\]](#).
- [20] J. Fan, L. Li, T. Liu, and K.-F. Lyu, “ W -Boson Mass, Electroweak Precision Tests and SMEFT,” [arXiv:2204.04805 \[hep-ph\]](#).
- [21] X. Liu, S.-Y. Guo, B. Zhu, and Y. Li, “Unifying gravitational waves with W boson, FIMP dark matter, and Majorana Seesaw mechanism,” [arXiv:2204.04834 \[hep-ph\]](#).
- [22] H. M. Lee and K. Yamashita, “A Model of Vector-like Leptons for the Muon $g - 2$ and the W Boson Mass,” [arXiv:2204.05024 \[hep-ph\]](#).
- [23] Y. Cheng, X.-G. He, Z.-L. Huang, and M.-W. Li, “Type-II Seesaw Triplet Scalar and Its VEV Effects on Neutrino Trident Scattering and W mass,” [arXiv:2204.05031 \[hep-ph\]](#).
- [24] E. Bagnaschi, J. Ellis, M. Madigan, K. Mimasu, V. Sanz, and T. You, “SMEFT Analysis of m_W ,” [arXiv:2204.05260 \[hep-ph\]](#).
- [25] A. Paul and M. Valli, “Violation of custodial symmetry from W -boson mass measurements,” [arXiv:2204.05267 \[hep-ph\]](#).
- [26] H. Bahl, J. Braathen, and G. Weiglein, “New physics effects on the W -boson mass from a doublet extension of the SM Higgs sector,” [arXiv:2204.05269 \[hep-ph\]](#).
- [27] P. Asadi, C. Cesarotti, K. Fraser, S. Homiller, and A. Parikh, “Oblique Lessons from the W Mass Measurement at CDF II,” [arXiv:2204.05283 \[hep-ph\]](#).
- [28] L. Di Luzio, R. Gröber, and P. Paradisi, “Higgs physics confronts the M_W anomaly,” [arXiv:2204.05284 \[hep-ph\]](#).
- [29] P. Athron, M. Bach, D. H. J. Jacob, W. Kotlarski, D. Stöckinger, and A. Voigt, “Precise calculation of the W boson pole mass beyond the Standard Model with FlexibleSUSY,” [arXiv:2204.05285 \[hep-ph\]](#).

- [30] J. Gu, Z. Liu, T. Ma, and J. Shu, “Speculations on the W-Mass Measurement at CDF,” [arXiv:2204.05296 \[hep-ph\]](#).
- [31] J. J. Heckman, “Extra W -Boson Mass from a D3-Brane,” [arXiv:2204.05302 \[hep-ph\]](#).
- [32] K. S. Babu, S. Jana, and V. P. K., “Correlating W -Boson Mass Shift with Muon $g - 2$ in the 2HDM,” [arXiv:2204.05303 \[hep-ph\]](#).
- [33] B.-Y. Zhu, S. Li, J.-G. Cheng, R.-L. Li, and Y.-F. Liang, “Using gamma-ray observation of dwarf spheroidal galaxy to test a dark matter model that can interpret the W -boson mass anomaly,” [arXiv:2204.04688 \[astro-ph.HE\]](#).
- [34] R. Balkin, E. Madge, T. Menzo, G. Perez, Y. Soreq, and J. Zupan, “On the implications of positive W mass shift,” [arXiv:2204.05992 \[hep-ph\]](#).
- [35] T. Biekötter, S. Heinemeyer, and G. Weiglein, “Excesses in the low-mass Higgs-boson search and the W -boson mass measurement,” [arXiv:2204.05975 \[hep-ph\]](#).
- [36] M. Endo and S. Mishima, “New physics interpretation of W -boson mass anomaly,” [arXiv:2204.05965 \[hep-ph\]](#).
- [37] A. Crivellin, M. Kirk, T. Kitahara, and F. Mescia, “Correlating $t \rightarrow cZ$ to the W Mass and B Physics with Vector-Like Quarks,” [arXiv:2204.05962 \[hep-ph\]](#).
- [38] K. Cheung, W.-Y. Keung, and P.-Y. Tseng, “Iso-doublet Vector Leptoquark solution to the Muon $g - 2$, R_{K,K^*} , R_{D,D^*} , and W -mass Anomalies,” [arXiv:2204.05942 \[hep-ph\]](#).
- [39] X. K. Du, Z. Li, F. Wang, and Y. K. Zhang, “Explaining The New CDFII W -Boson Mass In The Georgi-Machacek Extension Models,” [arXiv:2204.05760 \[hep-ph\]](#).
- [40] Y. Heo, D.-W. Jung, and J. S. Lee, “Impact of the CDF W -mass anomaly on two Higgs doublet model,” [arXiv:2204.05728 \[hep-ph\]](#).
- [41] N. V. Krasnikov, “Nonlocal generalization of the SM as an explanation of recent CDF result,” [arXiv:2204.06327 \[hep-ph\]](#).
- [42] Y. H. Ahn, S. K. Kang, and R. Ramos, “Implications of New CDF-II W Boson Mass on Two Higgs Doublet Model,” [arXiv:2204.06485 \[hep-ph\]](#).
- [43] X.-F. Han, F. Wang, L. Wang, J. M. Yang, and Y. Zhang, “A joint explanation of W -mass and muon $g-2$ in 2HDM,” [arXiv:2204.06505 \[hep-ph\]](#).
- [44] M.-D. Zheng, F.-Z. Chen, and H.-H. Zhang, “The $W\ell\nu$ -vertex corrections to W -boson mass in the R-parity violating MSSM,” [arXiv:2204.06541 \[hep-ph\]](#).
- [45] P. F. Perez, H. H. Patel, and A. D. Plascencia, “On the W -mass and New Higgs Bosons,” [arXiv:2204.07144 \[hep-ph\]](#).
- [46] A. Ghoshal, N. Okada, S. Okada, D. Raut, Q. Shafi, and A. Thapa, “Type III seesaw with R-parity violation in light of m_W (CDF),” [arXiv:2204.07138 \[hep-ph\]](#).
- [47] J. Kawamura, S. Okawa, and Y. Omura, “ W boson mass and muon $g - 2$ in a lepton portal dark matter model,” [arXiv:2204.07022 \[hep-ph\]](#).
- [48] K. I. Nagao, T. Nomura, and H. Okada, “A model explaining the new CDF II W boson mass linking to muon $g - 2$ and dark matter,” [arXiv:2204.07411 \[hep-ph\]](#).

- [49] S. Kanemura and K. Yagyu, “Implication of the W boson mass anomaly at CDF II in the Higgs triplet model with a mass difference,” [arXiv:2204.07511 \[hep-ph\]](#).
- [50] P. Mondal, “Enhancement of the W boson mass in the Georgi-Machacek model,” [arXiv:2204.07844 \[hep-ph\]](#).
- [51] K.-Y. Zhang and W.-Z. Feng, “Explaining W boson mass anomaly and dark matter with a $U(1)$ dark sector,” [arXiv:2204.08067 \[hep-ph\]](#).
- [52] D. Borah, S. Mahapatra, D. Nanda, and N. Sahu, “Type II Dirac Seesaw with Observable ΔN_{eff} in the light of W -mass Anomaly,” [arXiv:2204.08266 \[hep-ph\]](#).
- [53] T. A. Chowdhury, J. Heeck, S. Saad, and A. Thapa, “ W boson mass shift and muon magnetic moment in the Zee model,” [arXiv:2204.08390 \[hep-ph\]](#).
- [54] G. Arcadi and A. Djouadi, “The 2HD+a model for a combined explanation of the possible excesses in the CDF M_W measurement and $(g - 2)_\mu$ with Dark Matter,” [arXiv:2204.08406 \[hep-ph\]](#).
- [55] V. Cirigliano, W. Dekens, J. de Vries, E. Mereghetti, and T. Tong, “Beta-decay implications for the W -boson mass anomaly,” [arXiv:2204.08440 \[hep-ph\]](#).
- [56] E. Bagnaschi, M. Chakraborti, S. Heinemeyer, I. Saha, and G. Weiglein, “Interdependence of the new ”MUON G-2” Result and the W -Boson Mass,” [arXiv:2203.15710 \[hep-ph\]](#).
- [57] O. Popov and R. Srivastava, “The Triplet Dirac Seesaw in the View of the Recent CDF-II W Mass Anomaly,” [arXiv:2204.08568 \[hep-ph\]](#).
- [58] A. Bhaskar, A. A. Madathil, T. Mandal, and S. Mitra, “Combined explanation of W -mass, muon $g - 2$, $R_{K^{(*)}}$ and $R_{D^{(*)}}$ anomalies in a singlet-triplet scalar leptoquark model,” [arXiv:2204.09031 \[hep-ph\]](#).
- [59] M. Du, Z. Liu, and P. Nath, “CDF W mass anomaly in a Stueckelberg extended standard model,” [arXiv:2204.09024 \[hep-ph\]](#).
- [60] K. Ghorbani and P. Ghorbani, “ W -Boson Mass Anomaly from Scale Invariant 2HDM,” [arXiv:2204.09001 \[hep-ph\]](#).
- [61] L. M. Carpenter, T. Murphy, and M. J. Smylie, “Changing patterns in electroweak precision with new color-charged states: Oblique corrections and the W boson mass,” [arXiv:2204.08546 \[hep-ph\]](#).
- [62] E. Ma, “Verifiable radiative seesaw mechanism of neutrino mass and dark matter,” *Phys. Rev. D* **73** (2006) 077301, [arXiv:hep-ph/0601225](#).
- [63] M. Hirsch, R. A. Lineros, S. Morisi, J. Palacio, N. Rojas, and J. W. F. Valle, “WIMP dark matter as radiative neutrino mass messenger,” *JHEP* **10** (2013) 149, [arXiv:1307.8134 \[hep-ph\]](#).
- [64] I. M. Ávila, V. De Romeri, L. Duarte, and J. W. F. Valle, “Phenomenology of scotogenic scalar dark matter,” *Eur. Phys. J. C* **80** no. 10, (2020) 908, [arXiv:1910.08422 \[hep-ph\]](#).
- [65] **Particle Data Group** Collaboration, P. A. Zyla *et al.*, “Review of Particle Physics,” *PTEP* **2020** no. 8, (2020) 083C01.

- [66] **ATLAS** Collaboration, G. Aad *et al.*, “Observation of a new particle in the search for the Standard Model Higgs boson with the ATLAS detector at the LHC,” *Phys. Lett. B* **716** (2012) 1–29, [arXiv:1207.7214 \[hep-ex\]](#).
- [67] **CMS** Collaboration, S. Chatrchyan *et al.*, “Observation of a New Boson at a Mass of 125 GeV with the CMS Experiment at the LHC,” *Phys. Lett. B* **716** (2012) 30–61, [arXiv:1207.7235 \[hep-ex\]](#).
- [68] P. F. De Salas *et al.*, “Chi2 profiles from Valencia neutrino global fit,” 2021. <https://doi.org/10.5281/zenodo.4726908>.
- [69] J. A. Casas and A. Ibarra, “Oscillating neutrinos and $\mu \rightarrow e, \gamma$,” *Nucl. Phys. B* **618** (2001) 171–204, [arXiv:hep-ph/0103065](#).
- [70] A. Dedes and D. Karamitros, “Doublet-triplet fermionic dark matter,” *Physical Review D* **89** no. 11, (Jun, 2014) . <https://doi.org/10.1103/PhysRevD.89.115002>.
- [71] N. Khan, “Exploring the hyperchargeless Higgs triplet model up to the Planck scale,” *Eur. Phys. J. C* **78** no. 4, (2018) 341, [arXiv:1610.03178 \[hep-ph\]](#).
- [72] A. Abada and T. Toma, “Electric dipole moments in the minimal scotogenic model,” *JHEP* **04** (2018) 030, [arXiv:1802.00007 \[hep-ph\]](#). [Erratum: *JHEP* 04, 060 (2021)].
- [73] F. Staub, “Exploring new models in all detail with SARAH,” *Adv. High Energy Phys.* **2015** (2015) 840780, [arXiv:1503.04200 \[hep-ph\]](#).
- [74] W. Porod and F. Staub, “SPheno 3.1: Extensions including flavour, CP-phases and models beyond the MSSM,” *Comput. Phys. Commun.* **183** (2012) 2458–2469, [arXiv:1104.1573 \[hep-ph\]](#).
- [75] G. Bélanger, F. Boudjema, A. Pukhov, and A. Semenov, “micrOMEGAs4.1: two dark matter candidates,” *Comput. Phys. Commun.* **192** (2015) 322–329, [arXiv:1407.6129 \[hep-ph\]](#).
- [76] **XENON** Collaboration, E. Aprile *et al.*, “Dark Matter Search Results from a One Ton-Year Exposure of XENON1T,” *Phys. Rev. Lett.* **121** no. 11, (2018) 111302, [arXiv:1805.12562 \[astro-ph.CO\]](#).
- [77] J. Billard, L. Strigari, and E. Figueroa-Feliciano, “Implication of neutrino backgrounds on the reach of next generation dark matter direct detection experiments,” *Phys. Rev. D* **89** no. 2, (2014) 023524, [arXiv:1307.5458 \[hep-ph\]](#).
- [78] J. Billard *et al.*, “Direct Detection of Dark Matter – APPEC Committee Report,” [arXiv:2104.07634 \[hep-ex\]](#).
- [79] **LUX-ZEPLIN** Collaboration, D. S. Akerib *et al.*, “Projected WIMP sensitivity of the LUX-ZEPLIN dark matter experiment,” *Phys. Rev. D* **101** no. 5, (2020) 052002, [arXiv:1802.06039 \[astro-ph.IM\]](#).
- [80] **PandaX** Collaboration, H. Zhang *et al.*, “Dark matter direct search sensitivity of the PandaX-4T experiment,” *Sci. China Phys. Mech. Astron.* **62** no. 3, (2019) 31011, [arXiv:1806.02229 \[physics.ins-det\]](#).

- [81] M. E. Peskin and T. Takeuchi, “Estimation of oblique electroweak corrections,” *Phys. Rev. D* **46** (1992) 381–409.